Pergamon

Neural Networks, Vol. 10, No. 9, pp. 1571–1582, 1997

Printed in Great Britain
0893–6080/97 $17.00+.00

PII: S0893-6080(97)00075-0

CONTRIBUTED ARTICLE

The Population Vector, an Unbiased Estimator for Non-Uniformly Distributed Neural Maps

ROY GLASIUS, ANDRZEJ KOMODA AND STAN C. A. M. GIELEN

University of Nijmegen

(*Received* 3 *December* 1996; *accepted* 8 *July* 1997)

Abstract—*The Population Vector as a measure for the interpretation of neuronal activity in terms of sensory or motor events has been reliably used in the past for the case of uniformly distributed neuronal maps. In this study we will address the problem of the interpretation of neuronal activity in terms of the Population Vector for non-uniformly distributed maps. Based on mathematical analyses and on numerical computer simulations we demonstrate that, under some assumptions, the Population Vector also provides a proper estimate for neural maps with non-uniformly distributed neuronal response properties (i.e., the bias in the estimate, if present, is small). The main assumption is that the size of the receptive fields is not constant but that it is related to the density of receptive field properties. The confidence level of the results is expressed by the variance of the estimate in the limit of a large number of neurons.* © *1997 Elsevier Science Ltd. All rights reserved.*

Keywords—Neural networks, Population vector.

1. INTRODUCTION

In general, sensory and motor activity in biological neural networks is encoded by the activity of a large number of neurons. In order to provide insight in the representation of neuronal activity in motor cortex in monkey, Georgopoulos et al. (Georgopoulos, Kalaska, Crutcher, Caminiti, & Massey, 1984; Georgopoulos, Kettner, & Schwartz, 1986; Georgopoulos, Ashe, Smyrnis, & Taira, 1992) have formulated the hypothesis that the interpretation of motor activity in terms of planned movement direction could be estimated by a summation of the preferred directions of all neurons in an ensemble weighted by the firing rate of each single neuron. This weighted summation was defined as the Population Vector. A very similar approach was followed by Gielen, Hesselmans and Johannesma (1988) to interpret the neuronal activity in the cat auditory nerve. In their approach they simply replaced each action potential by the linear estimate of the impulse response of each neuron and summated the results for all neurons. The result of this approach was a Population Vector, which provided an estimate for the auditory stimulus, that caused the activity in the auditory nerve.

In addition to the Population Vector other approaches have been proposed (e.g., Abbot, 1994; Bialek & Rieke, 1988) to interpret neuronal activity. A frequently used method is the Maximum Likelihood Estimator which theoretically provides the optimal result. In order to compare the performance of the Maximum Likelihood Estimator and the Population Vector, Seung and Sompolinsky (1993) considered the theoretical case of a large set of neurons in visual cortex, each with a preferred direction, and studied the dependence of the performance on the variation of the size of the receptive fields of the neurons. In summary, they found that the Maximum Likelihood Estimator gave the best performance. However, the Population Vector appeared to be useful for several reasons, one of them being that the Population Vector is less sensitive to variations in the shape of the receptive field.

Most studies mentioned above explicitly or implicitly assumed a uniform distribution of preferred directions (or more generally, a uniform distribution of receptive field properties). However, non-uniform distributions of receptive field properties and preferred directions are a rule, rather than an exception in biological neural networks (see, for example, the receptive fields in superior colliculus (van Gisbergen, van Opstal, & Tax, 1987;

Acknowledgements: This work was partly supported by the Dutch Foundation for Neural Networks and by the Dutch Foundation for Scientific Research (NWO).

Requests for reprints should be sent to Prof. C. Gielen, Department of Medical Physics and Biophysics, University of Nijmegen, Geert Grooteplein Noord 21, 6525 EZ Nijmegen, The Netherlands. E-mail: stan@mbfys.kun.nl.

Rosa & Schmid, 1995) and in visual cortex (Hubel & Wiesel, 1962). As a result, direct application of the Population Vector to non-uniformly distributed neuronal maps may fail to give a proper estimate of the sensory or motor events, which are encoded in the neural activity.

In another study Salinas and Abbott (1994) proposed a linear reconstruction method, called the Optimal Linear Estimator, and tested this method on a set of neurons in visual cortex in order to reconstruct the stimulus orientation from measured firing rates. The latter method is based on a decorrelation of neuronal responses followed by weighted summation of the decorrelated responses. This method gives a faster convergence than the usual Population Vector. The decorrelation procedure, however, requires non-local operations in order to calculate the proper weight factor for the contribution of each cell, which makes it a biologically implausible method.

In this article we study the concept of a Population Vector for the case of non-uniformly distributed maps, and we demonstrate how an unbiased estimate of the interpretation of neuronal activity can be obtained under some mild assumptions. We start with some theoretical analyses, addressing the problem for non-uniformly distributed maps, to find an expression for the expectation value and its variance. We show that the Population Vector estimate in general is biased but that the bias is small or absent provided that a few assumptions are met. The Population Vector can be used to interpret neuronal activity, since the assumptions, which make the Population Vector applicable to non-uniformly distributed maps, are approximately met by most neural maps known in sensorimotor pathways. The theoretical results are illustrated by numerical simulations.

2. THEORY

Similarly to the earlier paper by Seung and Sompolinsky (1993) we will investigate the firing frequencies $r_1,\ldots, r_N$ of N simplified neurons in response to a stimulus θ_s. These neurons can be thought to be the so-called simple cells in area V1 of the visual cortex, which have an orientation sensitive receptive field (Hubel & Wiesel, 1962). Let us assume that $\theta_s \in [-\pi,\pi]$ is the orientation of a visual bar-like stimulus. The responses r_k of neurons are modeled by independent random variables with a Poisson probability distribution of the form

$$P(r_k;\theta_s)=\frac{f(\theta_s-\theta_k,a)^{r_k}}{r_k!}e^{-f(\theta_s-\theta_k,a)} \tag{1}$$

where $f(\theta_s-\theta_k,a) > 0$ is the mean response $\langle r_k\rangle$ of neuron k, θ_k is the preferred direction of neuron k and a is the width of the receptive field of a neuron. The mean firing frequency function is expressed by

$$f(\theta_s-\theta_k,a)=\begin{cases} f_{\min}+(f_{\max}-f_{\min})\cos^2\left(\frac{\pi}{a}(\theta_s-\theta_k)\right) & \text{if } |\theta_s-\theta_k|<a/2 \\ f_{\min} & \text{otherwise.}\end{cases} \tag{2}$$

Each neuron has a preferred direction $\theta_k \in [-\pi,\pi]$. When the stimulus θ_s is close to the preferred direction of the neuron, the probability of a large response r_k is high. If the stimulus is outside the receptive field of the neuron, the response is small with a mean firing rate $f_{\min}$.

We shall investigate the accuracy of the Population Vector estimate θ^* of an unknown stimulus θ_s. Unlike Seung and Sompolinsky (1993) we will consider non-uniform distributions of neurons assuming that the preferred directions θ_k of the neurons are distributed with a probability density $g(\theta)$. We chose for $g(\theta)$ a Gaussian distribution truncated to $[-\pi,\pi]$.

$$g(\theta)=\frac{\exp\left(\frac{-\theta^2}{2s^2}\right)}{\sqrt{2\pi s^2}\,\mathrm{erf}\left(\frac{\pi}{\sqrt{2}s}\right)} \tag{3}$$

Here, s is a real positive number and the error function is defined as $\mathrm{erf}(x)=\frac{2}{\sqrt{\pi}}\int_0^x \exp(-t^2)dt$. For large values of s the distribution approximates a uniform distribution, while for small values of s the density becomes sharply peaked for preferred directions near zero.

We use the complex number representation $z=e^{i\theta}$ for a two-dimensional vector (cos θ, sin θ). Keeping this in mind we define the Population Vector estimate as the weighted sum of preferred directions

$$z^*=\frac{1}{N\alpha}\sum_{k=1}^{N} r_k e^{i\theta_k} \tag{4}$$

where $\alpha \in R$ is a normalization factor chosen in such a way that z^* becomes a unit vector in the limit of large N. The estimate z^* is an unbiased estimate if its expectation value $\langle z^*\rangle$ is equal to $e_s^{i\theta}$, where $\langle\ldots\rangle$ represents the average with respect to the Poisson distribution (eqn (1)).

In Appendix A we have derived the following expression for the expectation value $\langle z^*\rangle$ for large N

$$\begin{aligned}\langle z^*(\theta_s)\rangle &= \frac{e^{i\theta_s}}{\alpha}\int_{-\pi}^{\pi} f(\phi,a)e^{i\phi}g(\phi+\theta_s)d\phi \\ &= \frac{e^{i\theta_s}}{\alpha}\int_{-\pi}^{\pi} f(\phi,a)\cos(\phi)g(\phi+\theta_s)d\phi \\ &\quad + i\frac{e^{i\theta_s}}{\alpha}\int_{-\pi}^{\pi} f(\phi,a)\sin(\phi)g(\phi+\theta_s)d\phi\end{aligned} \tag{5}$$

The expression for the estimated angle θ^* is given by

$$\theta^*=-i\ln\frac{\langle z^*\rangle}{|\langle z^*\rangle|}$$

Since the first integral at the right hand side of eqn (5) is

real valued, the first term in eqn (5) has always the same direction as the optimal estimate $\langle z^* \rangle = e^{i\theta_s}$. The second term is always orthogonal to the optimal estimate and, therefore, it represents the bias of the estimate.

For a uniform distribution of preferred directions the function $g(\phi)$ is constant ($g(\phi) = (2\pi)^{-1}$), which makes the second term in eqn (5) equal to zero because of the anti-symmetry of the sinus function. In this case the normalization factor α reduces to $\int_{-\pi}^{\pi} f(\phi, a)\cos(\phi)d\phi$ which is equal to the first Fourier transform $\tilde{f}_1$. This implies that an unbiased estimate is obtained for a uniform distribution of preferred directions.

For non-uniform distributions, the second term in eqn (5) will be different from zero in general. The relative magnitude of the first and second terms determines the effect of the bias in the estimate of the angle.

The considerations above show that the Population Vector estimator eqn (4) applied directly to non-uniformly distributed maps is in general a biased estimator. We shall show, however, that the Population Vector defined by eqn (4) can still be unbiased or, at least, that the bias will be sufficiently small, under some specific conditions.

The basic idea is that the bias will be small or zero, when the bias due to a changing density of preferred directions is compensated by a change in receptive field size. In detail, a bias induced by a larger number of neurons at one side of a stimulus due to a non-uniform distribution, could be compensated by reducing the size of the receptive field of these neurons, such that the number of neurons contributing to the Population Vector in the direction of higher density decreases with the result that the weighted summation of preferred directions is close to the stimulus value.

Therefore, we shall investigate the Population Vector for various combinations of distributions of preferred directions and of receptive receptive field sizes a. We shall demonstrate that for a particular choice of the function $a(\theta)$, namely when the receptive field size decreases for higher densities of preferred directions, the estimate θ^* deviates only slightly from the stimulus θ_s.

To find the optimal function $a(\theta)$ we define the following cost function:

$$C[a(\theta)] = \int_{-\pi}^{\pi} (\theta^*(a(\theta)) - \theta_s)^2 d\theta_s \qquad (6)$$

where θ^* is the Population Vector estimate for stimulus θ_s. The cost function is non-negative and for the unbiased estimate it has a minimal value equal to zero.

Our second goal is to find an expression for the standard deviation in the mean of the Population Vector estimate, which is represented by the variance of the estimate θ^*. An expression for this variance is derived in Appendix B (eqn (9)) and is given by

$$\sigma_\theta^2 = \frac{1}{N\alpha^2}\int_{-\pi}^{\pi} f(\phi, a)\sin^2(\phi)g(\phi + \theta_s)d\phi$$

For a uniform distribution $g(\phi) = (2\pi)^{-1}$ the variance reduces to

$$\sigma_\theta^2 = \frac{1}{N\tilde{f}_1^2}\int_{-\pi}^{\pi} f(\phi, a)\left[\frac{1}{2} - \frac{1}{2}\cos(2\phi)\right]\frac{d\phi}{2\pi} = \frac{\tilde{f}_0 - \tilde{f}_2}{2N\tilde{f}_1^2}$$

as derived earlier by Seung and Sompolinsky (1993). Here $\tilde{f}_n \equiv \int_{-\pi}^{\pi} f(\phi, a)e^{-in\phi}d\phi$ is the nth order Fourier transform of f.

3. NUMERICAL SIMULATIONS

In the numerical simulations we consider a sample of $N = 1000$ neurons with preferred directions drawn from the interval $[-\pi, \pi]$ with the probability density given by eqn (3). For a finite number of neurons N the expectation value for z^* and the variance σ_θ^2 are given by

$$\langle z^*(\theta_s)\rangle = \frac{1}{N\alpha}\sum_{k=1}^{N} f(\theta_k - \theta_s; a(\theta_k))e^{i\theta_k}$$

$$\sigma_\theta^2 = \frac{1}{N^2\alpha^2}\sum_{k=1}^{N} f(\theta_k - \theta_s; a(\theta_k))\sin^2(\theta_k - \theta_s)$$

where

$$\alpha = \frac{1}{N}\sum_{k=1}^{N} f(\theta_k; a(\theta_k))\cos(\theta_k)$$

Note that this normalization factor gives a unit vector when the bias is zero, i.e., in the case of a uniform distribution of preferred directions, or when $\theta_s = 0$. The orientation of the estimate does not depend on the normalization factor α. In our simulations we use $f_{\min} = 10$ and $f_{\max} = 1000$.

The task now is to find a function $a(\theta)$ which minimizes the cost function eqn (6).

A search procedure for a function $a(\theta)$ without any constraints is a difficult variational problem since it requires to look for a minimum of the cost function in the space of all functions for which the integral exists. Therefore, we restrict our search to functions which are polynomials in θ_k. Because $a(\theta_k)$ has to be larger than zero and because the distribution eqn (3) is symmetric around zero we choose

$$a(\theta_k) = \sum_{l=0}^{L} c_l|\theta_k|^l$$

Neurons with preferred direction θ_k and $-\theta_k$ should have the same width of receptive fields because of the symmetric shape of $g(\theta)$. We use a set of stimuli which are uniformly distributed between -3.1 and 3.1 with step size 0.1 to find $a(\theta)$ which minimizes the cost function averaged over all stimuli

$$\theta_{s_i} \in \{-3.1, -3.0, ..., 3.0, 3.1\}$$

Our problem now reduces to minimization of the cost

function

$$C(\{c_l\}) = \sum_i (\theta^*(\theta_{s_i}) - \theta_{s_i})^2 \qquad (7)$$

with L unknown coefficients c_l. We look for the unknown coefficients c_l in the L-dimensional cube $[-1,1]^L$ using a method of simulated annealing (Kirkpatrick, Gelatt, & Vecchi, 1983). This optimization technique is well accepted to find the minimum in an energy landscape as defined by eqn (7). It provides the opportunity to escape from local minima because steps to higher values of the energy function are allowed with a finite probability.

3.1. The Uniform Distribution

Figure 1 presents the mean of the variance over 10^3 stimuli in the estimate $z^*(\theta)$ as a function of the receptive field width a for two values for the number of neurons ($N = 10^3$, 10^4). Clearly there is an optimum for values near 0.8 radian. This value for a is similar to the result obtained in previous studies (Seung & Sompolinsky, 1993; Gielen, Glasius, & Komoda, 1996) and corresponds to the receptive field width which gives the optimum in the amount of information in the neural activity.

This result can be understood from the following. For values of a near zero each neuron responds very selectively and many stimuli will not elicit any stimulus related neuronal activity at all. As a consequence the number of neurons responding to stimuli is small and the variance in the Population Vector due to the stochastic nature of the actionpotentials is large for very small values of a. For large values of a almost all neurons will respond to almost any stimulus. Hence, the accuracy to estimate the proper stimulus will be low and the variance will be large.

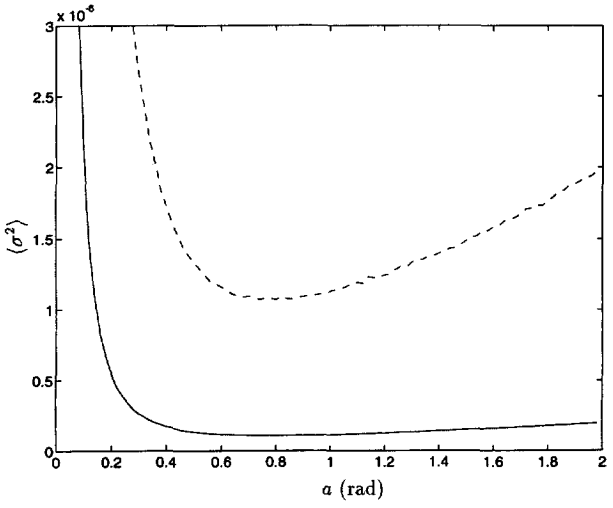

FIGURE 1. The mean variance $\langle\sigma^2\rangle$ of the Population Vector estimate (averaged over 10^3 trials) as a function of the receptive field width a for $N = 10^3$ (dashed line) and $N = 10^4$ (solid line) for homogeneously distributed preferred directions of the neurons.

A larger number of neurons gives a smaller variance corresponding to a better estimate of the stimulus. The minimum in the variance shifts to smaller values of a for a larger number of neurons.

3.2. The Non-Uniform Distribution

The results for a non-uniform distribution are shown in Figure 2. In this simulation, the Gaussian distribution of preferred directions, as defined in eqn (3), has a standard deviation s equal to one radian. If we minimize the cost function eqn (7) by using the search algorithm outlined before, we find the set of receptive field widths $\{a_k\}$ shown in Figure 2a. The optimal values for a_k in the range between -2 and $+2$ radian vary by 1.2 radian and increase rapidly outside this range. Values for a receptive field width larger than 10 are not shown. The largest receptive width was found for preferred directions near π and $-\pi$ and appeared to be as large as 1800. Figure 2b (solid line) shows the bias when the receptive fields are not constant but change as shown in Figure 2a. For comparison, we included the results when a constant value for a, which was optimal for the whole set of neurons, was chosen for all neurons (dashed line). For the former case (receptive field size related to density of preferred directions) the bias is much smaller over the whole range. However, the bias is not zero and the estimate can be missed by 0.2 radian. The corresponding variance in the estimate of the Population Vector is shown in Figure 2c.

The oscillations in Figure 2b are due to variations in the number of contributing neurons with a relatively broad tuning in the regions $[-2, -1.5]$ and $[1.5, 2]$. Therefore, and because of the low density of neurons in the outer regions, these oscillations can be considered to be a boundary artifact. In order to exclude these artifacts we have adjusted the cost criterion eqn (7) in such a way that we look for the distribution of receptive field widths which minimize the bias in the estimate, only in the region which contains 95% of the total number of neurons. For the Gaussian distribution with standard deviation $s = 1$, the stimulus region is $[-2,2]$ rad. Hence, we took the sum in eqn (7) over this segment for $\theta_{si} \in \{-2.0, -1.9, \ldots, 1.9, 2.0 \text{ (rad)}\}$. Note that we allow all neurons to contribute to the estimate for the proper stimulus.

Figure 3 shows the results of this analysis for the truncted cost criterion for the same Gaussian distribution ($s = 1$ rad). We have stopped the search procedure when the estimates differ less than 0.0075 radian from the true value, i.e., when $\forall_{\theta_{s_i}} : |\theta^*(\theta_{s_i}) - \theta_{s_i}| < 0.0075$. Figure 3a shows the optimal distribution of receptive field widths. Figure 3b (solid line) shows that with respect to the result in Figure 2b the new distribution shown in Figure 3a gives a bias which is significantly reduced in the interval $[-2,2]$ radian. The dashed line in Figure 3b shows the bias for the case with the same (optimal) receptive field

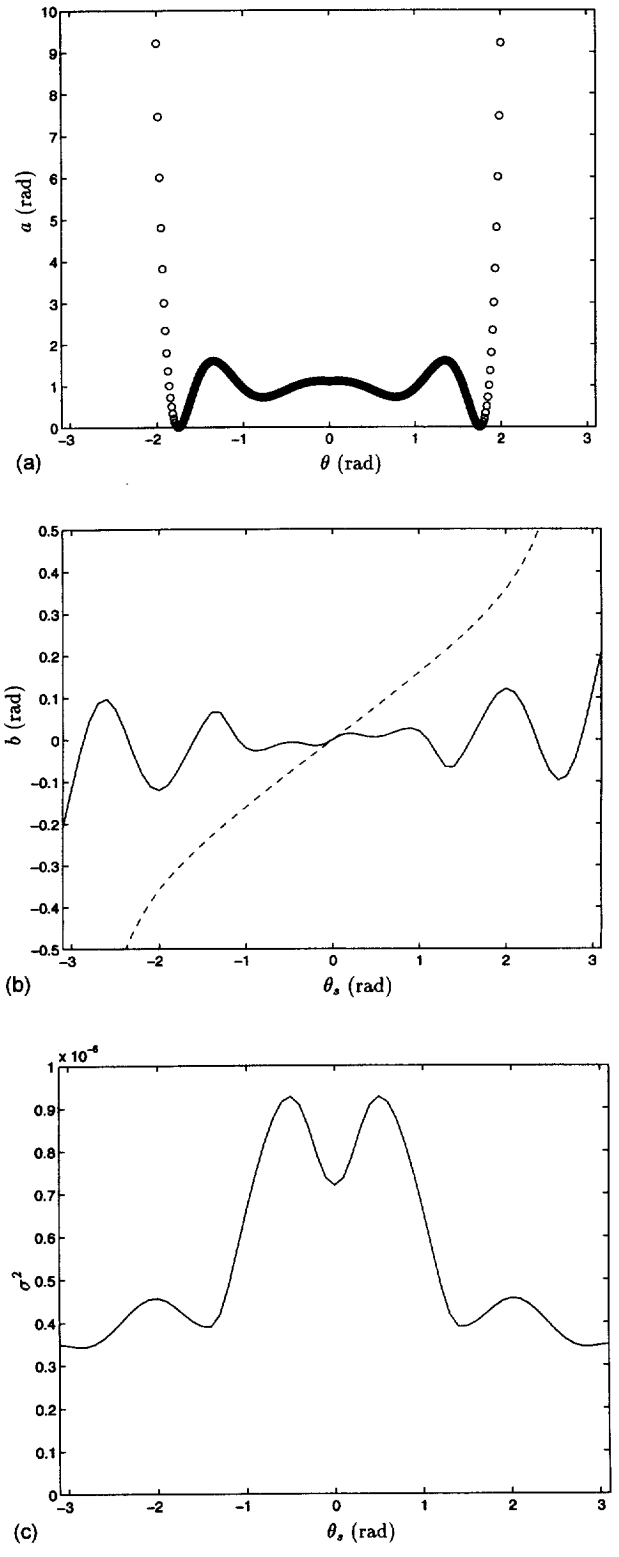

FIGURE 2. The results of a numerical simulation with distribution $g(\theta)$ and $s = 1.0$ and $N = 1000$. (a) The optimal width a for neurons with various preferred directions. For each neuron the combination (θ_k, a_k) is indicated with an open dot. Receptive field widths larger than ten are not displayed. (b) The bias $b(\theta^*)$ in the estimate as a function of the stimulus value θ_s (solid line). In the case of an optimal constant receptive field width for all neurons, i.e., $a = 1.1$ (dashed line). (c) The variance of the Population Vector for stimulus values θ_s.

width for all neurons, as in Figure 2b. The variance in the range from -2 to $+2$ radian is small (Figure 3d) and is comparable to the variance shown in Figure 2c. Figure 3c illustrates that the optimization procedure gives receptive field widths which are smaller for higher densities.

To illustrate the fact that contributions of neurons with a preferred direction far from the stimulus value can contribute to a reduction of the bias we present the results of Figure 3 in an alternative way in Figure 4. In Figure 4a we have calculated the mean firing frequency for some stimuli $\theta_s \in [0,\pi]$ and for all neurons. Figure 4b is a cross section of Figure 4a, where the mean firing frequency of all neurons is shown for the case $\theta_s = 0$. The graph is symmetric. Near the stimulus value $\theta_s = 0$ a group of neurons responds and "votes" for an estimate near zero. However, also in the far regions near π and $-\pi$ some neurons with large receptive field widths respond to the stimulus. Because of the symmetry however, the total contribution to the estimate is zero. Hence an unbiased estimate $\theta^* = 0$ is the result.

When the stimulus orientation is $\theta_s = 0.2$, there is a cluster of responding neurons with preferred directions near $\theta_s = 0.2$ and a group of neurons with preferred directions near π and $-\pi$ (Figure 4c). Note that the cluster of neurons with a preferred direction near $\theta_s = 0.2$ is symmetric with a large number of responding neurons with preferred directions near zero due to the larger density of preferred directions near $\theta_s = 0$. This asymmetry causes a bias in the Population Vector, which is offset by the somewhat larger group of responding neurons with a preferred direction near π. As a result, the bias in the Population Vector is small (Figure 3b, solid line). For a stimulus value $\theta_s = 1$ (Figure 4d) the two groups of responding neurons overlap.

The occurrence of two disconnected groups of responding neurons does not agree with experimental data (van Gisbergen et al., 1987; Hubel & Wiesel, 1962; Rosa & Schmid, 1995) which report only one group of responding neurons. In fact the large receptive field widths near the extremes $-\pi$ and π are an artifactual boundary effect. Therefore, additional constraints have to be formulated in order to find results which will meet the experimental results. We regard the group of neurons with a preferred direction equal to or close to the stimulus value as the main group. Neurons do not belong to the main group if their response $f(\theta_s - \theta_k, a_k)$ is larger than the response of the neighboring neuron which has a preferred direction closer to the stimulus. We replace the mean firing frequencies of all the neurons not belonging to the main group by the minimal mean firing frequency value $f_{\min}$. The width of the receptive field a has been adjusted so as to minimize the bias.

Figure 5 shows the result of the constrained search algorithm. The bias in the estimate θ^* is slightly larger in Figure 5b than in Figure 3b. Figure 5c shows that the optimal distribution of receptive fields corresponds to

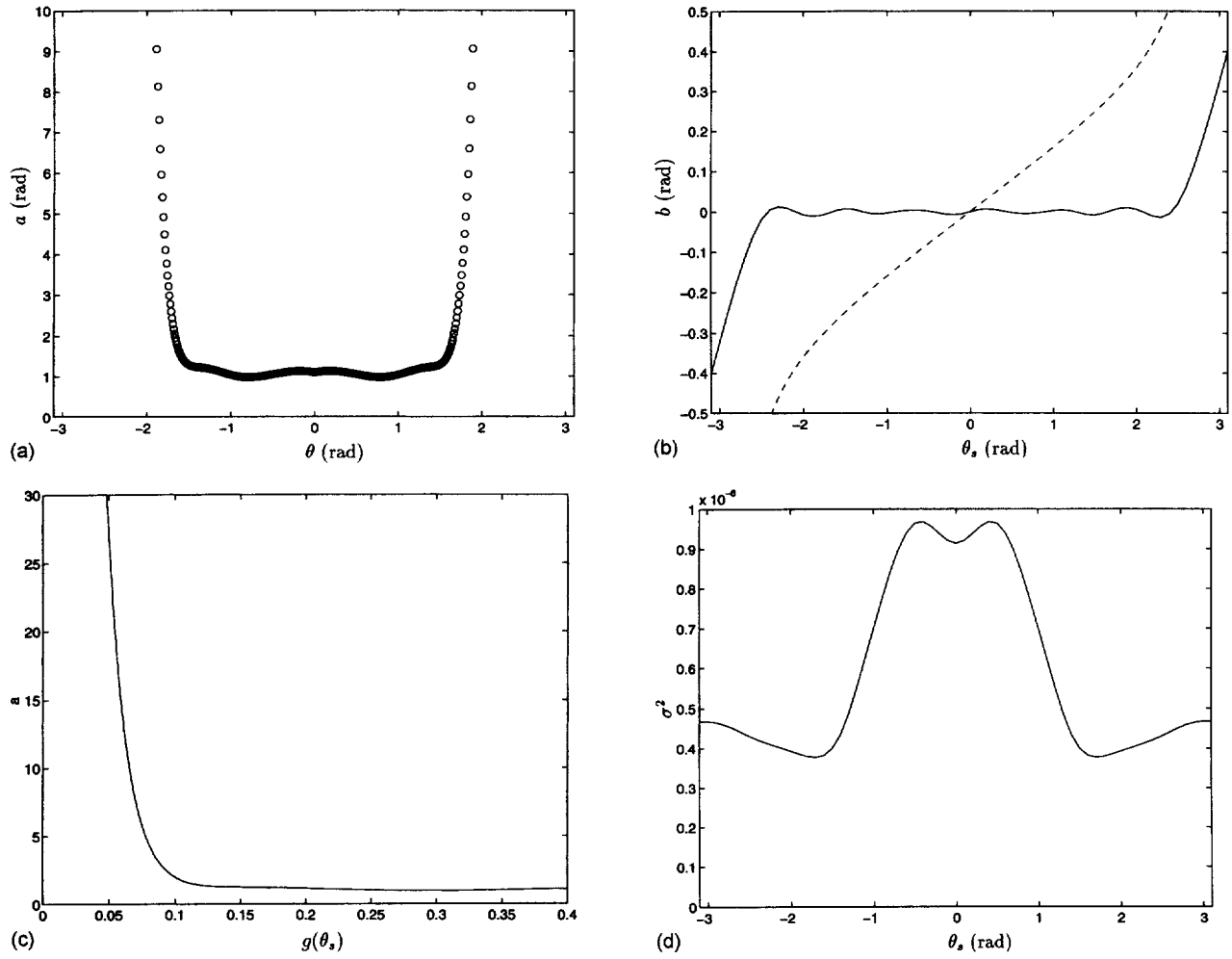

FIGURE 3. The results of the numerical simulations with distribution $g(\theta)$ with $s = 1.0$ (rad), $N = 1000$. The cost is integrated over the interval $\theta_s \in [-2.0, 2.0]$. (a) The optimal width a for neurons as a function of preferred direction. For each neuron the combination (θ_k, a_k) is indicated with an open dot. Receptive field widths larger than 10 are not displayed. (b) The bias $b(\theta^*)$ in the estimate as a function of the stimulus value θ_s (solid line) and for the case of an optimal constant receptive field width for all neurons ($a = 1.1$, dashed line). We have stopped the search procedure when each estimate differs less than 0.0075 radian from the true value, i.e., when $\forall_{\alpha s \beta}: |\theta^*(\theta_{s\beta}) - \theta_{s\beta}| < 0.0075$. (c) The optimal receptive field width $a(\theta)$ as a function of the density $g(\theta)$. (d) The variance of the Population Vector for various stimulus values θ_s.

smaller receptive field widths for higher densities of neurons. Due to the smaller receptive field width of neurons at higher densities the number of neurons with a preferred direction smaller and larger than the stimulus value is approximately constant giving rise to the relatively small bias in Figure 5b. The variance in the Population Vector estimate is slightly larger in Figure 5d than in Figure 3d.

The firing rate of the neurons responding to various stimuli is shown in Figure 6. For all stimuli a single cluster of neurons is responding. Notice that the cluster of responding neurons is smaller than in Figure 5. This is related to the fact that the width of the receptive fields for this model in the range of preferred directions $[-1,1]$ is smaller than for the model shown in Figure 3.

3.3. Robustness for Variations in Receptive Field Width

Although there is a general tendency for neurons in the visual system and in the auditory system to have smaller receptive fields when the density of neurons is higher (in accordance with the result in Figure 5c) there is a considerable variability in receptive field width. Therefore, we have investigated the robustness of the Population Vector estimate for deviations of the optimal receptive field width as shown in Figure 5c. The results are shown in Figure 7.

Multiplication of all receptive field widths by a factor of 1.5 did not have a large effect on the bias (compare Figure 5b and Figure 7a). This illustrates that it is the relative size of receptive field widths which is important to minimize the bias in the Population Vector estimate, rather than absolute size of the receptive field width.

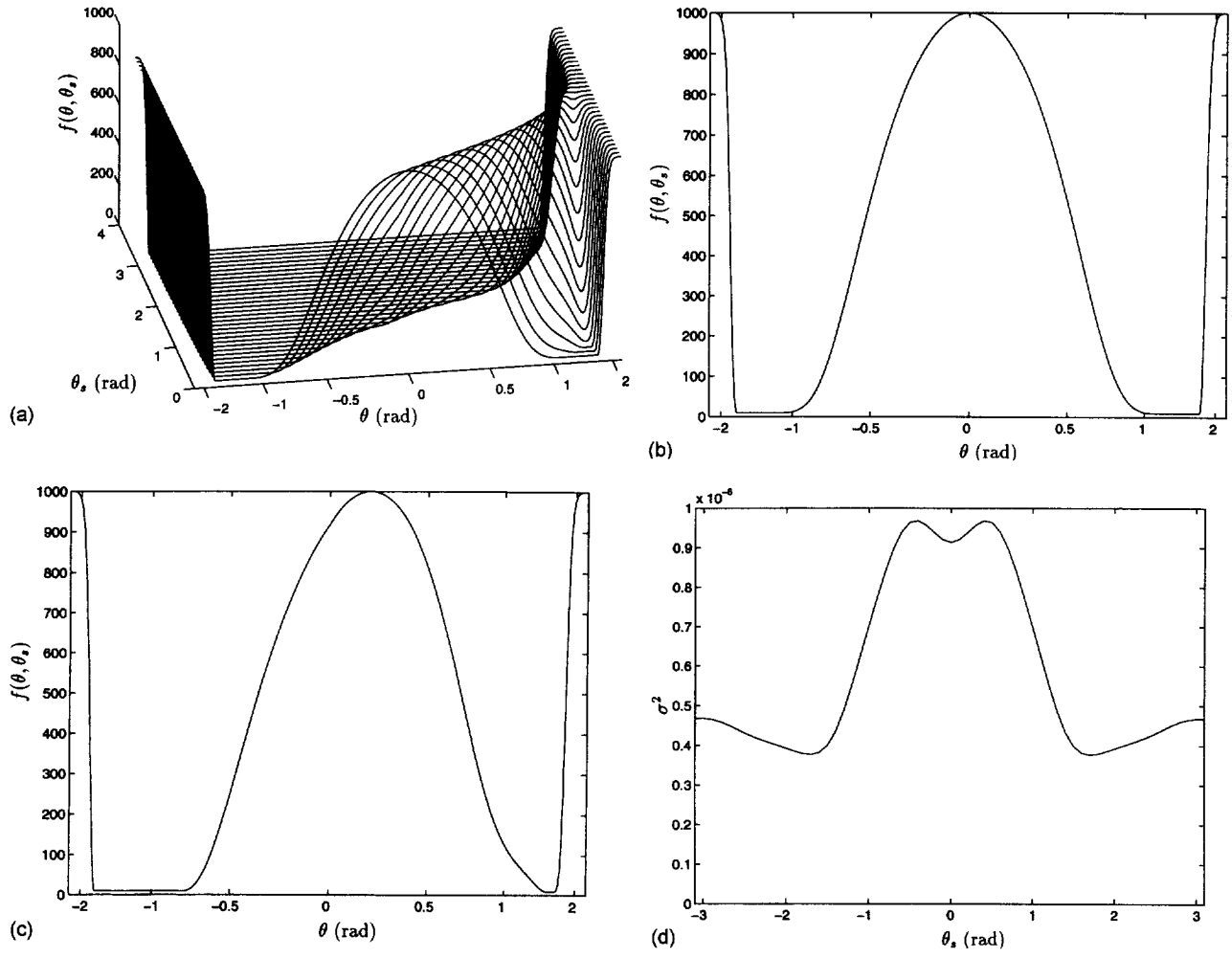

FIGURE 4. (a) The mean firing frequency of neurons versus the preferred direction of each neurons for some stimuli θ_s. $N = 1000$ and $s = 1.0$. (b) Cross section of (a) for $\theta_s = 0$. (c) Cross section of (a) for $\theta_s = 0.2$. (d) Cross section of (a) for $\theta_s = 1$. Note that the θ-axis is scaled in a way such that the density of neurons along the axis becomes uniform.

The Population Vector estimate is also robust for random variations in the receptive field width a. Inducing a variability in receptive field width by multiplication of each a-value by the uniformly distributed random variable z in the interval [0,5] for each neuron has only a small effect on the bias (compare Figure 5b and Figure 7b).

Simulations in which the density of preferred directions was randomly modified by 25% also demonstrated that the bias and variance remained the same within 5% in the interval [−2,2].

4. DISCUSSION

The Population Vector coding has been a popular way of interpreting neuronal activity. However, this method has frequently been associated with the assumption of homogeneous sampling of the input space by neurons. The main result of this study is that the Population Vector can also provide an accurate estimate of the sensorimotor event when the distribution of receptive field properties is not homogeneously distributed. In that case the Population Vector can provide an accurate result if there is an approximately inverse relation between the receptive field width and the density of receptive fields. Random variations in receptive field properties do have a small effect only on the Population Vector estimate, presumably because the variations in the contribution of cells due to the variations in receptive field width disappear in the summation of the contributions of all responding neurons.

In this discussion we will first concentrate on the question, whether the assumptions, which underlie our method, are in agreement with experimental observations. After that, we will discuss the significance and relevance of the results of this paper in the context of previous publications.

In the visual system it is well known that the density of receptive fields is much higher near the fovea than it is towards the periphery. This has been found both in retina

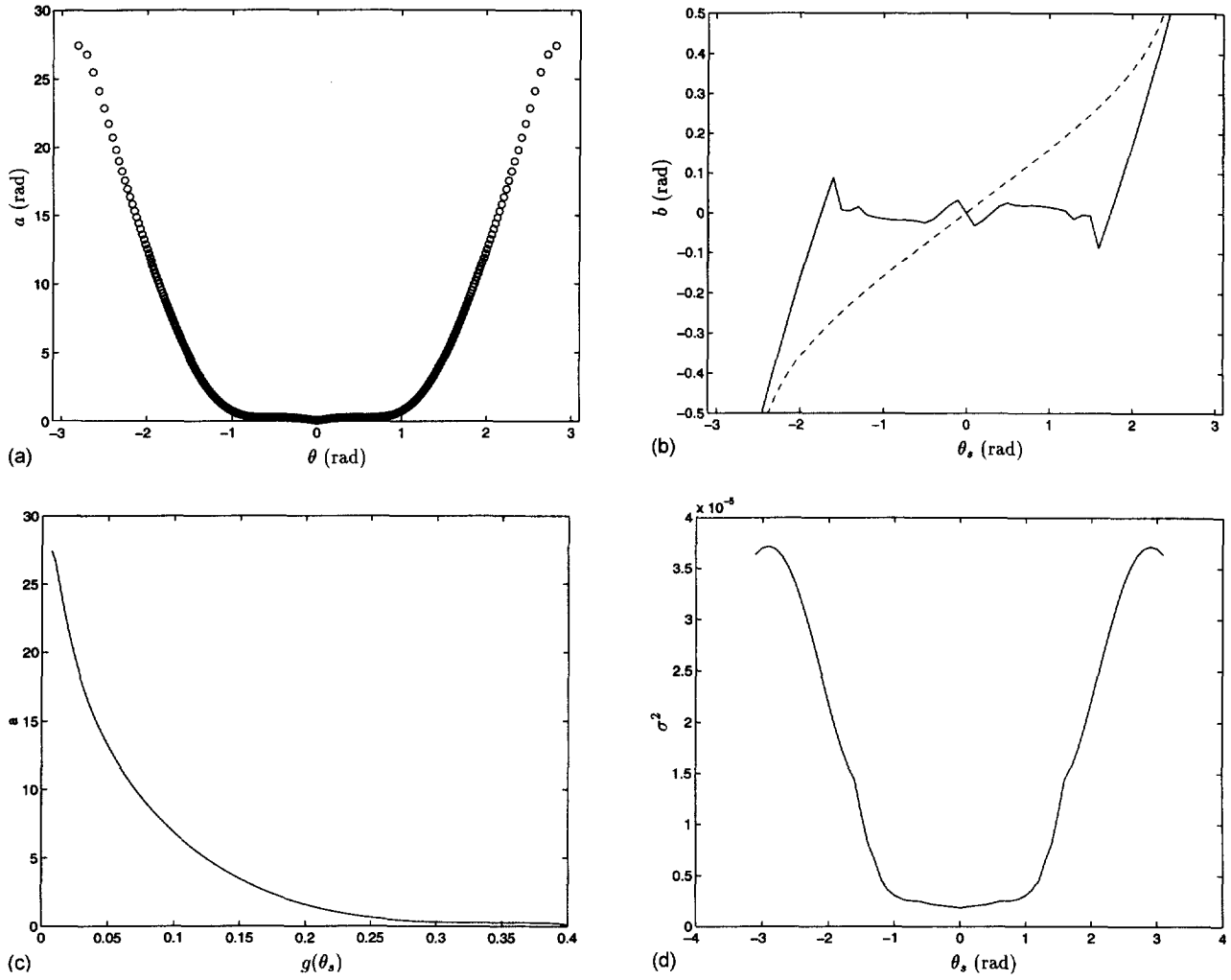

FIGURE 5. The results of a numerical simulation with distribution $g(\theta)$ and $s = 1.0$, $N = 1000$ and with the constraint of one single responding group of neurons. The cost is integrated over the interval $\theta_s \in [-2.0, 2.0]$. (a) The optimal width a for neurons with various preferred directions. For each neuron the combination (θ_k, a_k) is indicated with an open dot. (b) The bias $b(\theta_s)$ in the estimate as a function of the stimulus value θ_s (solid line). In the case of an optimal constant receptive field width for all neurons, i.e., $a = 1.1$ the bias is indicated by the dashed line. (c) The optimal receptive field width $a(\theta)$ as a function of the density $g(\theta)$. (d) The variance of the Population Vector for various stimulus values θ_s.

(Peichle & Wässle, 1979) and in visual cortex (Peichle, Wässle, Grünert, Rohrenbeck, & BoycottPeichle et al., 1990; Rovamo & Virsu, 1984; Schwartz, 1980), where the density of receptive fields decreases exponentially towards the periphery. The fact that a larger part of visual cortex is devoted to the central visual field is summarized by the cortical magnification factor (Rovamo & Virsu, 1984; Schwartz, 1980; van Essen, Newsome, & Mannsellvan Essen et al., 1984). It is also a well known fact, that the mean receptive field size increases from the fovea towards the periphery in retina (Peichle & Wässle, 1979) and visual cortex (van Essen et al., 1984). In cat retinal ganglion cells the receptive field size of the center is approximately inversely related to the density of receptive fields (Peichle & Wässle, 1979). In monkey visual cortex the receptive field size decreases with the inverse of the cortical magnification factor (van Essen et al., 1984). These literature data indicate that, qualitively, the receptive field size and density of receptive fields in retina and cortex are inversely related, as suggested by the results of this study.

Based on studies using electrical stimulation (Robinson, 1972) van Gisbergen et al. (1987) proposed a logarithmic function to describe the mapping from retinal coordinates to the coordinates in the superior colliculus. This logarithmic function implies that the density of neurons decreases exponentially towards the periphery, like in visual cortex. The receptive field size was assumed to be constant in collicular coordinates based on the findings of McIlwain (1975). This implies that the receptive field size increases logarithmically in retinal coordinates (i.e., with the inverse of the exponential

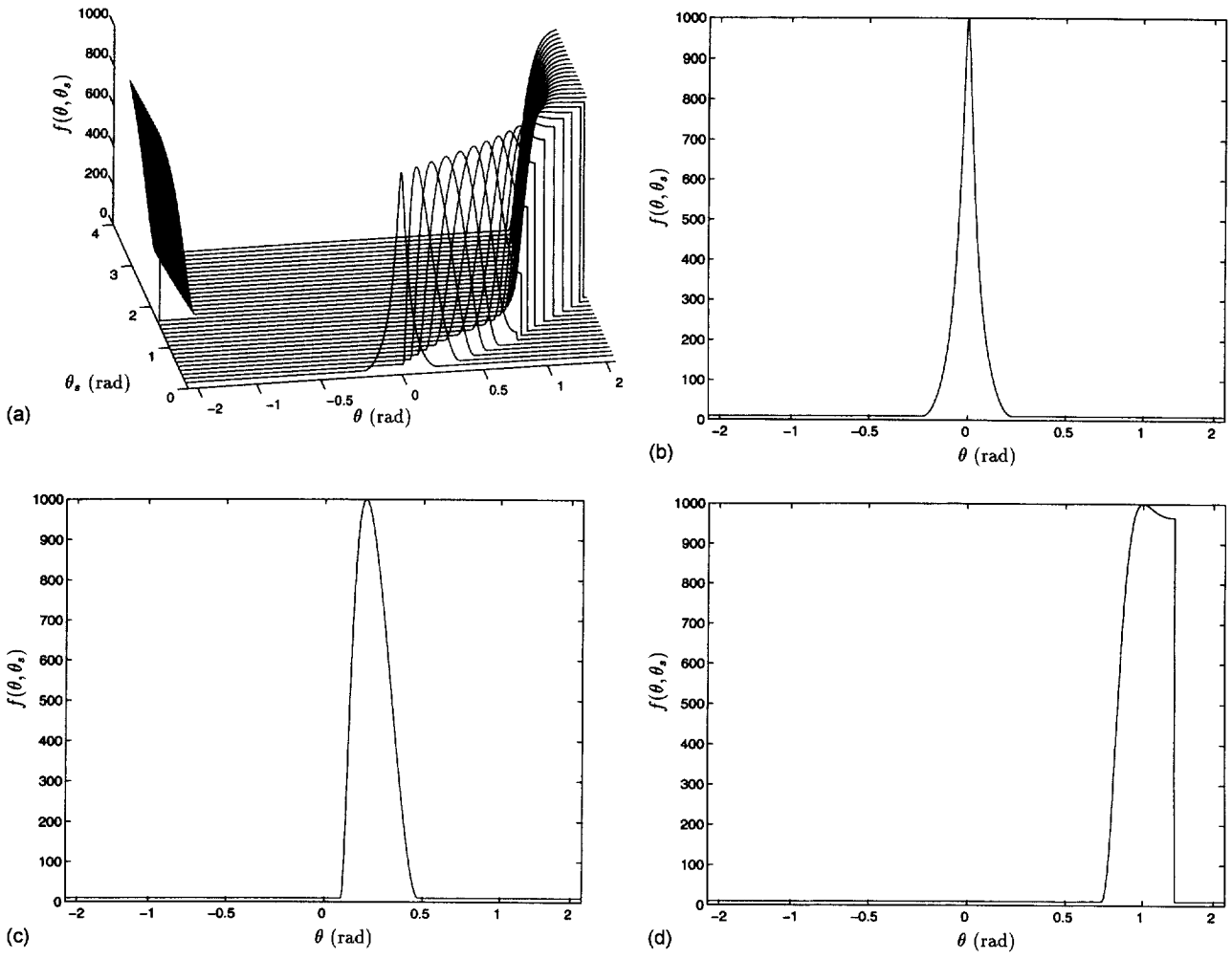

FIGURE 6. (a) The mean firing frequency of the neurons versus the preferred direction of the neurons for some stimuli θ_s. $N = 1000$, $s = 1.0$. The constraint was imposed that only one group of neurons was responding for each stimulus. (b) Cross section of (a) for $\theta_s = 0$. (c) Cross section of (a) for $\theta_s = 0.2$. (c) Cross section of (a) for $\theta_s = 1$. Note that the θ-axis is scaled in a nonlinear way such that the density of neurons along that axis is uniform.

density function). Due to this inverse relationship of the functions which describe density and receptive field size of neurons as a function of retinal eccentricity, the population estimate of collicular activity in van Gisbergen et al. (1987) gave a reliable, unbiased estimate of target position in space.

In the auditory system, the distribution of fibers in the acoustic nerve is ordered as a function of frequency. The density of fibers is highest at the higher frequencies and decreases for lower frequencies (Kiang, 1965). The equivalent of the receptive field size for auditory nerve fibers, the width of the frequency tuning curve or the inverse of the sharpness of tuning, is smaller for nerve fibers tuned at high frequencies (i.e., when the density of fibers is high) and increases for lower frequencies (Kiang, 1965). The fact that the Population Vector could be used to provide a sensory interpretation of the stimulus related activity in the acoustic nerve with its non-uniform distribution of tuning curves (see Gielen et al., 1988) was possible thanks to the inverse relation between density of neurons and tuning curve of neurons. These examples of previous studies, which have successfully used the Population Vector ideas for cases of non-uniformly distributed receptive fields supports the theoretical ideas outlined in this study.

The problem that a non-uniform distribution of receptive fields might give rise to artifactual results for the Population Vector has been recognized before in other studies. Salinas and Abbott (1994) presented a method which corrects for the correlation in firing rate of neurons caused by the fact that the optimal stimulus is not orthogonal for different neurons. This method also corrects for non-uniformities in the distribution of neurons and in addition gives a better signal-to-noise ratio than the well known Population Vector. This method is certainly a good way to interpret the neuronal activity. Whether or

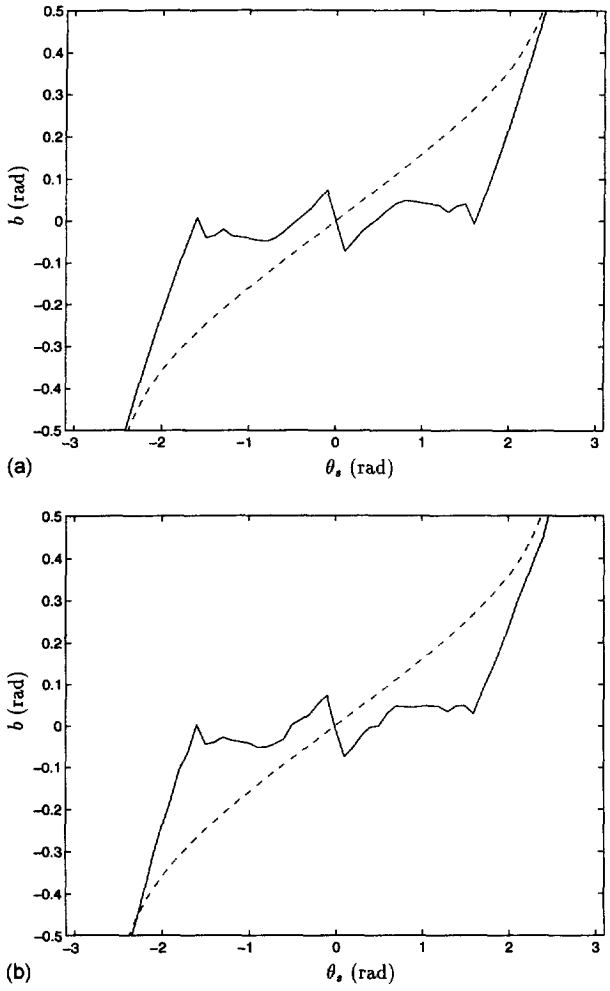

FIGURE 7. The bias $b(\theta^*)$ in the estimate as a function of the stimulus value θ_s (solid line), where $N = 1000$, $s = 1.0$, and with the constraint of one responding group for each stimulus. The dashed line represents the bias in the case of an optimal constant receptive field width for all neurons ($a = 1.1$). (a) The parameter a has been multiplied by 1.5 for all neurons. (b) The parameter a has been multiplied by z randomly chosen from the interval [0,5].

not this method is also of relevance for our understanding of neuronal information processing in biological neural networks remains an open question, since this procedure requires non-local operations on neuronal activity information, which is in general assumed to be non-realistic from a biological point of view. Since motocortical cells are known to have monosynaptic contacts with motorneurons of distal muscles (Porter & Lemon, 1977) the advantage of the Population Vector is that it bears more resemblance with the way in which activity in motor cortex becomes evident for external observation as the summation of motor-unit twitches, which give rise to force and movements.

The search procedure to find the optimal value for the parameters a (which corresponds to half the receptive field width) gives a value of about 1.1 radian (Figure 3a), which is close to the optimal value of 0.8 radian in Figure 1. However, it should be noted that the optimal a-value in Figure 1 is found by minimization of the variance σ^2, whereas the optimal a-values shown in Figure 3a are found by minimization of the bias. Apparently, both procedures give similar results.

When the restriction is imposed that only one group of neurons responds to each stimulus, the optimal a-value appears to become somewhat smaller. We also found that multiplication of all receptive field widths by the same constant does hardly affect the bias (see Figure 7a). This can be understood from the data in Figure 1, which shows that the curvature in the minimum of the variance as a function of a is rather small. As a consequence, the same variations in a for all neurons will not have a large impact on the variance of the estimate. Therefore, different constraints on the model give rise to different values for the optimal a-value without large effects on the variance.

Random variations in the receptive field width hardly affect the Population Vector estimate either. This is mainly because any effects of the random variations in receptive field width disappear by adding the responses of many responding neurons. For stimulus values near π and $-\pi$ the averaging effect is smaller due to the smaller density of neurons. Hence, variations in a give rise to a larger bias and variance for smaller densities of neurons.

In summary, we conclude that the Population Vector can be used as an estimate for the sensory or motor interpretation of neural activity for non-uniform maps when the density of receptive field properties and receptive field are inversely related. The latter assumption seems to be in agreement with present knowledge about neuronal information processing in most sensory systems.

REFERENCES

Abbot, L.F. (1994). Decoding neuronal firing and modeling neural networks. *Quarterly Review of Biophysics, 27,* 291–331.

Bialek, W., & Rieke, F. (1988). Reliability and information transmission in spiking neuron. *Trends in Neurosciences, 15,* 428–433.

van Essen, D.C., Newsome, W.T., & Mannsell, J.H.R. (1984). The visual field representation in straiate cortex of the macaque monkey: Assymtries, anisotropies and individual variability. *Vision Research, 24,* 429–448.

Georgopoulos, A.P., Kalaska, J.F., Crutcher, M.D., Caminiti, R., & Massey, J.T. (1984). The representation of movement direction in the motor cortex: single cell and population studies. In G.M. Edelman, W.E. Gail & W.M. Cowan (Eds.), *Dynamic aspects of neocortical function* (pp. 501–524). Neurosciences Research Foundation.

Georgopoulos, A.P., Kettner, R.E., & Schwartz, A. (1986). Neural population coding of movement directions. *Science, 243,* 234–236.

Georgopoulos, A.P., Ashe, J., Smyrnis, N., & Taira, M. (1992). The motor cortex and the coding of force. *Science, 256,* 1692–1695.

Gielen, C.C.A.M., Hesselmans, G.H.F.M., & Johannesma, P.I.M.

(1988). Sensory interpretation of neural activity patterns. *Mathematical Biosciences, 88,* 15–35.

Gielen, C.C.A.M., Glasius, R., & Komoda, A. (1996). Interpretation of neuronal activity in neural networks. *Journal of Neurocomputing, 12,* 249–266.

van Gisbergen, J.A.M., van Opstal, A.J., & Tax, A.M.M. (1987). Collicular ensemble coding of saccades based on vector summation. *Neuroscience, 21,* 541–555.

Hubel, D.H., & Wiesel, T.N. (1962). Receptive fields, binocular interaction and functional architecture in the cat's visual cortex. *Journal of Physiology, 160,* 106–154.

Kiang, N. (1965). *Discharge patterns of single fibers in the cat's auditory nerve.* Cambridge: M.I.T.

Kirkpatrick, S., Gelatt, C.D., & Vecchi, M.P. (1983). Optimization by simulated annealing. *Science, 220,* 671–680.

McIlwain, J.T. (1975). Visual receptive fields and their images in superior colliculus of the cat. *Journal of Neurophysiology, 20,* 535–538.

Peichle, L., & Wässle, H. (1979). Size, scatter and coverage of ganglion cell receptive field centres in the cat retina. *Journal of Physiology, 291,* 117–141.

Peichle, L., Wässle, H., Grünert, U., Röhrenbeck, J., & Boycott, B.B. (1990). Retinal ganglion cell density and cortical magnification factor in the primate. *Vision Research, 30,* 1897–1911.

Porter, R., & Lemon, R. (1977). *Corticospinal neurones. Their role in movement.* London: Academic.

Robinson, D.A. (1972). Eye movements evoked by collicular stimulation in the alert monkey. *Vision Research, 12,* 1795–1808.

Rosa, M.G.P., & Schmid, L.M. (1995). Magnification factors, receptive field images and point-image size in the superior colliculus of flying foxes: Comparison with the primary visual cortex. *Experimental Brain Research, 102,* 551–556.

Rovamo, J., & Virsu, V. (1984). Isotropy of cortical magnification and topography of striate cortex. *Vision Research, 24,* 283–286.

Salinas, E., & Abbott, L.F. (1994). Vector reconstruction from firing rates. *Journal of Computational Neuroscience, 1,* 89–107.

Schwartz, E.L. (1980). Computational anatomy and functional architecture of striate cortex: A spatial mapping approach to perceptual coding. *Vision Research, 20,* 645–669.

Seung, H.S., & Sompolinsky, H. (1993). Simple models for reading neuronal population codes. *Proceedings of the National Academy of the Sciences of the USA, 90,* 10749–10753.

APPENDIX A: THE EXPECTATION VALUE $\langle z^* \rangle$

In this appendix we derive an analytical expression for the expectation value of the Population Vector estimate for the case of non-uniformly distributed preferred directions.

$$\langle z^* \rangle = \left\langle \frac{1}{Nn} \sum_{k=1}^{N} r_k e^{i\theta_k} \right\rangle$$

$$= \frac{1}{Nn} \sum_{\theta_k=\theta_1}^{\theta_N} f(\theta_k - \theta_s, a) e^{i\theta_k}$$

If N is large the sum can be replaced by an integral

$$\langle z^* \rangle = \frac{1}{\alpha} \int_{-\pi}^{\pi} f(\theta - \theta_s, a) e^{i\theta} g(\theta) d\theta$$

Changing variables $\phi = \theta - \theta_s$ and assuming a symmetric function of the density of preferred directions results into

$$\langle z^* \rangle = \frac{e^{i\theta_s}}{\alpha} \int_{-\pi}^{\pi} f(\phi, a) e^{i\phi} g(\phi + \theta_s) d\phi$$

$$= \frac{e^{i\theta_s}}{\alpha} \left(\int_{-\pi}^{\pi} f(\phi, a) \cos(\phi) g(\phi + \theta_s) d\phi + i \int_{-\pi}^{\pi} f(\phi, a) \sin(\phi) g(\phi + \theta_s) d\phi \right)$$

APPENDIX B: VARIANCE OF THE DIRECTIONAL FLUCTUATIONS

For large N z^*, as a sum of independent random variables, has a two-dimensional Gaussian distribution. This distribution is completely determined the correlation matrix

$$C = \begin{pmatrix} \langle (x - \bar{x})^2 \rangle & \langle (x - \bar{x})(y - \bar{y}) \rangle \\ \langle (x - \bar{x})(y - \bar{y}) \rangle & \langle (y - \bar{y})^2 \rangle \end{pmatrix} \tag{8}$$

where $x = \mathrm{Re}\vec{z}$ and $y = \mathrm{Im}\vec{z}$.

To calculate the variance in z^* we define

$$\begin{cases} x \equiv \mathrm{Re}(z^*) = \dfrac{1}{Nn} \displaystyle\sum_{k=1}^{N} r_k \cos(\theta_k) \\ y \equiv \mathrm{Im}(z^*) = \dfrac{1}{Nn} \displaystyle\sum_{k=1}^{N} r_k \sin(\theta_k) \end{cases}$$

Using the shorthand notation $f_k = f(\theta_k - \theta_s, a)$, the variance in x is

$$\langle (x - \bar{x})^2 \rangle = \left\langle \left(\frac{\sum_{k=1}^{N} r_k \cos(\theta_k)}{Nn} - \frac{\sum_{k=1}^{N} f_k \cos(\theta_k)}{Nn} \right)^2 \right\rangle$$

$$= \frac{1}{N^2 \alpha^2} \left\langle \left(\sum_{k=1}^{N} (r_k - f_k) \cos(\theta_k) \right)^2 \right\rangle$$

$$= \frac{1}{N^2 \alpha^2} \left\langle \sum_{k=1}^{N} (r_k - f_k)^2 \cos(\theta_k)^2 + \sum_{k \neq l}^{N} (r_k - f_k)(r_l - f_l) \cos(\theta_k) \cos(\theta_l) \right\rangle$$

$$= \frac{1}{N^2 \alpha^2} \left\langle \sum_{k=1}^{N} (r_k - f_k)^2 \cos(\theta_k)^2 \right\rangle$$

$$= \frac{1}{N^2 \alpha^2} \sum_{k=1}^{N} f_k \cos^2(\theta_k)$$

In the latter two steps we use the fact that $(r_k - f_k)$ are independent random variables and the fact that $< (r_k - f_k)^2 > = \sigma_{r_k}^2 = f_k$.

Likewise we calculated the variance in y and the covariance

$$\langle (y - \bar{y})^2 \rangle = \left\langle \left(\frac{\sum_{k=1}^{N} r_k \sin(\theta_k)}{Nn} - \frac{\sum_{k=1}^{N} f_k \sin(\theta_k)}{Nn} \right)^2 \right\rangle$$

$$= \frac{1}{N^2 \alpha^2} \sum_{k=1}^{N} f_k \sin^2(\theta_k)$$

$$\langle (x - \bar{x})(y - \bar{y}) \rangle = \left\langle \left(\frac{\sum_{k=1}^{N} r_k \cos(\theta_k)}{Nn} - \frac{\sum_{k=1}^{N} f_k \cos(\theta_k)}{Nn} \right) \times \left(\frac{\sum_{k=1}^{N} r_k \sin(\theta_k)}{Nn} - \frac{\sum_{k=1}^{N} f_k \sin(\theta_k)}{Nn} \right) \right\rangle$$

$$= \frac{1}{N^2 \alpha^2} \sum_{k=1}^{N} f_k \cos(\theta_k) \sin(\theta_k)$$

The two eigenvalues of the matrix correspond to eigenvectors, in the direction of the orientation θ and in the direction of the magnitude $R = |z^*|$. Hence the fluctuations in θ are given by the eigenvalue corresponding to the eigenvector in the direction θ. It is equal to

$$\sigma_\theta^2 = \frac{1}{N\alpha^2}\int_{-\pi-\theta_s}^{\pi-\theta_s} f(\phi, a)\left[\frac{1}{2} - \frac{1}{2}\cos(2\phi)\right] g(\phi+\theta_s)d\phi \qquad (9)$$

$$= \frac{1}{N\alpha^2}\int_{-\pi-\theta_s}^{\pi-\theta_s} f(\phi, a)\sin^2(\phi) g(\phi+\theta_s)d\phi$$